Design and characterization of a low-profile haptic system for telemanipulation

C.F. Blanco-Diaz†, G. Degl'Innocenti†, E. Vendrame, M. Uliano, M. Controzzi and L. Cappello

***Abstract*—In telemanipulation, supplementary feedback can enhance operator perception and control precision. This study introduces a haptic interface designed to convey temporally discrete tactile cues when remotely controlling a robot. Low-profile piezoelectric sensors were integrated in the thumb of a robotic hand to capture the key events of the manipulation task (i.e., object contact and release). Synchronously with such events, pressure bursts were delivered to the operator's fingertip through a soft textile thimble equipped with inflatable pockets. Both this haptic display and the sensing module were individually evaluated. The pneumatic system responsible for pockets inflation was characterized in terms of reaction time, proving suitable for the application with a latency of less than 70 ms. Regarding the sensing module, the behavior of the sensorized thumb was first evaluated under static conditions, identifying contact and release events when grasping with the robotic hand differently shaped objects fixed on a table. Then, the accuracy of the touch event detection was assessed while performing a more complex manipulation task (i.e., a pick and lift task). This evaluation was conducted first with the robot programmed to grasp and lift an object following pre-defined trajectories, where we measured accuracy of 100% for contact and 90% for release event detection. Then, we performed a telemanipulation pilot study involving eight participants, where the system proved capable of correctly detecting object contact and release events with an accuracy of 100% and 86.4%. Despite preliminary, these results confirmed proper functioning of the system and paved the way for the exploration of a new haptic feedback policy in telemanipulation based on temporally discrete tactile events.**

***Index Terms*— Haptic interfaces, human-robot interaction, pneumatic actuators, telerobotics, wearable devices**

I. INTRODUCTION

In recent decades, robots are becoming more and more pervasive in our society [1]. Among them, robotic platforms for teleoperation gained recognition thanks to their ability of performing tasks remotely and in hazardous environments, such as demining, disarming ordnances, handling radioactive materials, and carrying out surgical operations [2] [3].

To effectively operate a telerobot, the human operator must have available sufficient information about the status of the robot and its interaction with the surrounding environment, i.e., proprioceptive and exteroceptive information [1][2]. The most common approach to convey proprioceptive information in telemanipulation is through vision, i.e., the operator observes the robot movements, either through direct observation or via remote cameras. However, vision doesn't allow to capture exteroceptive information, which is paramount to manipulate objects with confidence and dexterity [4]. It stands to reason that providing supplementary exteroceptive (e.g., tactile) information would improve telemanipulation performances.

Conversely, it is only recently that the literature demonstrated the efficacy of supplementary tactile feedback in telemanipulation [5]. Possibly, this is because equipping the robot and the operator respectively with haptic sensors and stimulators is burdensome in terms of costs, encumbrance and complexity [1]. Moreover, it is generally agreed that providing supplementary feedback is not a trivial task [6][7].

According to the Discrete Event-driven Sensorimotor Control (DESC) theory, the Central Nervous System (CNS) monitors the progress of the manipulation task through the achievement of task subgoals marked by temporally discrete mechanical events corresponding to the transient events of the task (i.e., object contact, lift-off, replace, and release) [4][8][9]. If these events are artificially signaled to the brain, e.g., using short-lasting mechanical stimuli in sensitive areas, individuals can rapidly integrate such temporally discrete feedback in their sensorimotor control with minimal cognitive burden [8]. Vibrotactile and electrotactile feedback strategies have been extensively investigated to elicit haptic sensations [5][10]. It should be noted that vibrotactile and electrotactile feedback strategies have been found to be effective in prosthetics, characterized by non-somatotopic arrangements (i.e., the feedback is applied on different anatomical parts than those initiating the action) [8]. This could be a limit in telemanipulation where somatotopic feedback is expected by the user [10]. This imposes a technological burden, as the actuators/electrodes must be miniaturized to the size of a fraction of a fingertip. An alternative to these strategies is represented by pneumatic systems, as they ensure great compatibility with teleoperation setups as the bulky components (pneumatic pumps, solenoid valves, etc.) are conveniently placed off board, while the user in only required

This work was co-funded by INAIL (the Italian National Workers' compensation) under the HANDeVAL project (G.A. PR23-SV-P1). The work of L.C. was co-funded by the European Union (ERC, MUSE, G.A. 101116249). Views and opinions expressed are however those of the author(s) only and do not necessarily reflect those of the European Union or the European Research Council. Neither the European Union nor the granting authority can be held responsible for them. MC is supported by the Italian Ministry of Research, under the PNNR action "THE-Tuscany Health Ecosystem" – Spoke 9 (project number ECS 00000017).

C.F. Blanco-Diaz, G. Degl'Innocenti, E. Vendrame, M. Uliano, M. Controzzi and L. Cappello are with the BioRobotics Institute, Scuola Superiore Sant'Anna, Pisa, Italy; and with the Department of Excellence in Robotics and AI, The BioRobotics Institute, Scuola Superiore Sant'Anna, Pisa, Italy. (leonardo.cappello@santannapisa.it)

†These authors contributed equally to this work

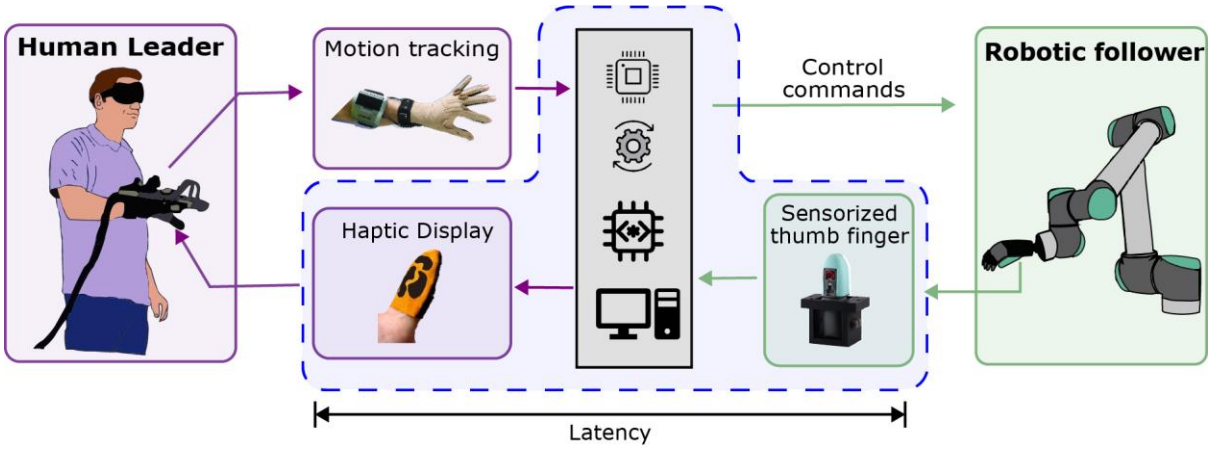

Fig. 1. Block diagram of the proposed teleoperation system, where the human leader controls a robotic follower. The latter composed of a robotic arm with an anthropomorphic hand as end-effector, whose thumb was instrumented with custom piezoelectric sensors. The leader controls the follower through an off-the-shelf motion capture system and wears a custom textile-based pneumatic haptic display. A controller detects tactile events and translates them into discrete pressure stimuli. Blue dashed lines outline the original contribution of this work.

to wear pneumatic actuators on their fingertips. Moreover, a pneumatic platform provides homo-modal feedback (i.e., it renders a pressure event with a pressure stimulus) that could be seamlessly integrated by the user [11].

Furthermore, instrumenting a robotic platform is non-trivial, given the complexity of gathering tactile information during dexterous robotic manipulation. Different sensing technologies are currently being developed for teleoperation, demonstrating the cogency of this topic [10]-[14].

To implement a feedback policy based on the DESC theory, we recently proposed the use of piezoelectric sensors in a wearable device to detect the key events of the manipulation task [9]. This sensing technology, which have the twofold advantage of being extremely lightweight and sensitive, proved sufficiently streamlined and accurate for the application. In this work, we propose a low-profile haptic system to return discrete tactile feedback during telemanipulation, exploiting the same sensing technology. In the context of a typical teleoperation platform comprising a leader (i.e., a human operator) and a follower (i.e., a robot), the main contribution of this work concerned: i) the sensorization of the follower (i.e., a robotic hand) to allow the detection of the crucial tactile events of the manipulation task (i.e., object contact and release), ii) the development of a wearable haptic display, and iii) the implementation of a controller to allow the user to close the control loop based on tactile information (Fig. **1**). We sought to keep the system as streamlined as possible; to this aim, ultra-thin custom piezoelectric sensors were embedded in the thumb finger of a robotic hand, while a haptic display leveraging textile-based fluidic actuators was devised. We characterized the components of this system on the benchtop and in a telemanipulation scenario to verify their functionality, with promising results.

II. Material and Methods

A. *Robotic Hand Sensorization*

For our telemanipulation system, we employed a dexterous robotic hand (Mia Hand, Prensilia s.r.l.), which we instrumented to detect contact and release events. To this aim, ultra-thin piezoelectric sensors based on polyvinylidene-fluoride (PVDF) were incorporated in its thumb, the finger involved in the majority of the grasps (i.e., it is opposable to the other fingers). To determine adequate placement and number of sensors, we leveraged the results of a previous study that identified the frequency maps of the contact points of the thumb of the robotic hand Mia while grasping standard objects (Fig. **2**) [14]. We manufactured three custom sensors (S1, S2, S3 - Fig. **2**) by outlining and smoothing the areas of the thumb where contact frequency was greater than zero. Since the areas of the power grasp and the pinch grasp were overlapping, we subtracted the area of L3 (corresponding to the pinch grasp) from the area of L1 (power grasp), which was wider. The area of L2 (lateral grasp) did not overlap with the other two. The sensors' shapes obtained from the aforementioned procedure were cut out from a commercial PVDF sheet (1-1004347-0, TE Connectivity Measurement Specialties) and treated as in [9] to ensure robust connection. The response of the PVDF sensors was previously characterized by applying and removing known external forces using a three-dimensional moving platform equipped with a triaxial load cell [9]. These sensors produce significant positive (negative) voltage spikes upon contact

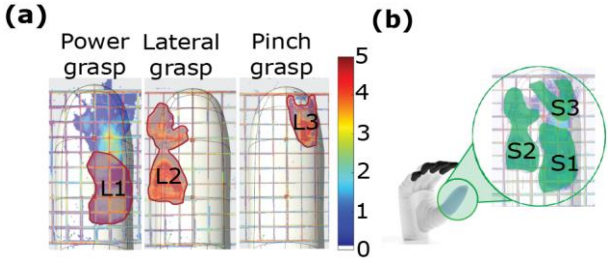

Fig. 2. (a) Frequency maps of contact of the robotic thumb obtained during different grasps– power, lateral, and pinch – and outline of the contact areas (note that L1 is reduced to avoid overlap with L3). (b) Final shape and location of the sensors into the sensorized thumb of Mia Hand.

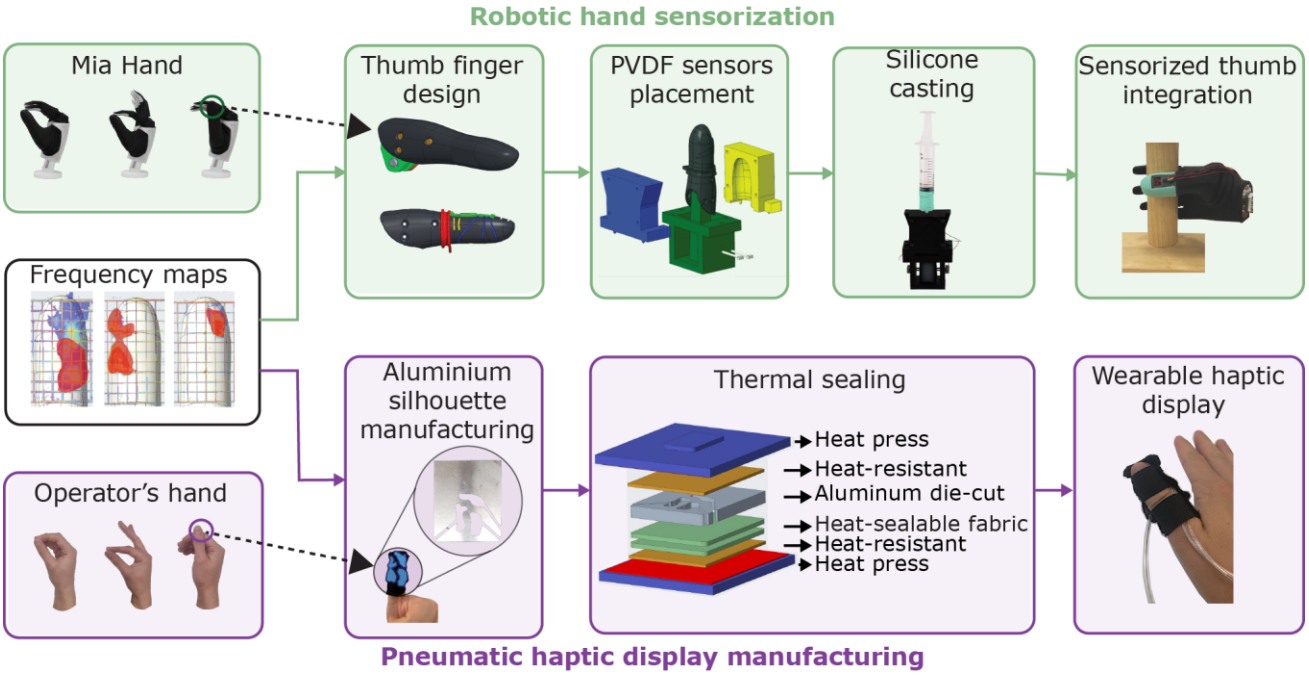

Fig. 3. Manufacturing process of the sensorized thumb with PDVF-based piezoelectric sensors (upper portion) and of the textile-based wearable haptic display (lower portion). It is worth noting that the contact frequency maps of [14] were used as a reference to design the shape of the sensors and the pneumatic actuators.

(release) events, due to their high sensitivity toz mechanical deformation. The sensors were then positioned on the internal structure (bone) of the robotic thumb, which was redesigned to facilitate their integration and 3D printed with SLS techniques. Finally, this customized bone with the sensors attached to its external surface was covered with a silicone skin (Smooth-Sil 960, Smooth On, USA) to encapsulate and protect them from the external environment (Fig. **3**).

B. Haptic Display Manufacturing

We devised a soft pneumatic haptic display consisting of a textile thimble with three textile-based inflatable pockets. Each pocket was meant to inflate synchronously with the touch events detected by the corresponding sensor placed in the robotic thumb, providing somatotopic pressure cues at the fingertip (Fig. **2**). To fabricate them, we layered two identical sheets of airtight, heat-sealable fabric and an aluminum silhouette. This silhouette consisted of a 3 mm-thick rectangular aluminum block where we carved through-holes with shapes similar to the sensors described in the previous paragraph, by means of CNC machining. These shapes were smoothed and modified to have a minimum distance of 2 mm between the pockets to increase robustness (which is compatible with the tactile acuity of the fingertips [14]). This stack was placed in the heat press, protected by two sheets of heat-resistant foil, at a temperature of 145 °C for 25 s (Fig. **3** – Pneumatic haptic display manufacturing). As a result, the two fabrics were sealed together only where in contact with the aluminum body that conducted heat, while the empty areas prevented thermal sealing, resulting in three airtight pockets. We then connected these pockets to T2 pneumatic tubing.

C. Control Architecture

Our control system comprised three solenoid valves (VZ110-5MOZ-M5-Q, RS Components) connected to a wall-mounted pneumatic outlet regulated at 100 kPa. Each valve was driven by a motor driver (L298N Dual H-Bridge), controlled by a custom electronic board based on a 16-bit microcontroller (PIC24F16KL401-I/MQ, Microchip Technology Inc.). The board acquired the three sensors signals, which were amplified, sampled with a 10-bit ADC, and processed with a detection algorithm for identifying contact and release events during object manipulation. After an event was detected on a sensor, the corresponding pocket on the thimble was inflated for a duration of 160 ms, which was empirically determined to be easily perceivable. To avoid multiple detections, we set a refractory period of 320 ms after each event is detected, during which further events are ignored, akin to [9]. The detection algorithm was built with a State Machine (SM) logic based on threshold-crossing rules. The states and the transition rules of the algorithm are summarized below

- *Idle State*. The system starts idling. The current state switches to Contact State if the sensor signal crosses a positive threshold ($ThrC_1$).
- *Contact State*. The contact event is detected. In this state, the sensor signal is filtered with a moving average filter (40 ms time window) to reduce the noise caused by sustained contact with the object. The current state switches to the Release State when the sensor signal crosses a negative threshold (*ThrR*) or switches back to the Idle State in case of a flat sensor signal for 2000 ms (i.e., within the idle thresholds – *ThIs*).

- *Release State*. The release event is detected. The moving average filter is removed. A negative threshold (*ThrR*) and a larger positive threshold ($ThrC_2$) are set to detect other possible contact or release events, respectively. It is worth noting that unintentional collisions with the object and slippages may occur in this state, which may cause false activations: for this reason, we increased the contact threshold. The current state switches back to Idle State in case the signal lays flat within the *ThIs* for 2000 ms.

The thresholds were determined with an automated calibration procedure before each use of the system through a dedicated graphical user interface. The calibration method is described in [16].

III. Experimental Setup and Data Analysis

To characterize and assess the performance of the system, each component (haptic display and sensorized thumb) was tested with different procedures.

First, we assessed the reaction time of the haptic display to secure adequate responsiveness, as minimal delay is acceptable for haptic rendering [7][17]. Subsequently, we mounted the sensorized robotic hand on a 6-axis industrial robotic arm (UR5, Universal Robot) to preliminary evaluate the sensors response when the hand grasped objects in static conditions (e.g., the robotic arm did not move). Finally, the performance of the sensorized hand was assessed in two dynamic conditions: (1) with the robotic arm programmed to follow pre-defined trajectories and (2) in a real teleoperation scenario.

A. Haptic display latency

In this test we assessed the latency of the haptic display, defined as time delay between a digital control command and the onset of pocket inflation. To detect this onset, we fixed a vibrational sensor (1028414-00, TE Connectivity Measurement Specialties) on a bench and connected the haptic display to the sensor with bi-adhesive tape to capture its deformation caused by inflation. The digital control command and the vibrational sensor signal were synchronized and acquired through an oscilloscope (WAVESURFER 3014Z, Teledyne LeCroy). Upon deformation, the vibrational sensor responded with a voltage peak. The time delay between the control command and the voltage peak of the activation onset was computed over 25 trials.

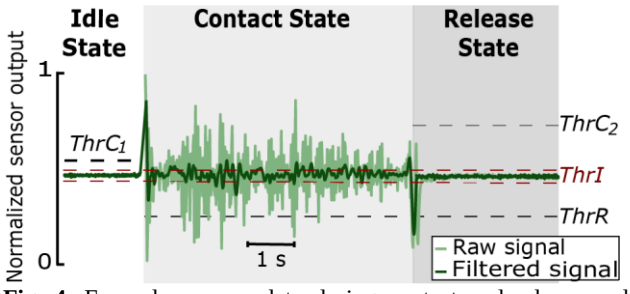

Fig. 4. Exemplar sensor data during contact and release and relative state transitions of the proposed control architecture. Raw and filtered data are shown for comparison. Dotted lines represent the thresholds for state transition.

B. Static evaluation of the sensorized thumb

The performance of the sensorized thumb was preliminarily evaluated during static object grasping. The robotic hand was programmed to grasp a series of objects fixed on a table, while the robotic arm kept the hand with the correct orientation with respect to the objects. Depending on the shape of the object, the robotic hand was programmed to perform one of the Mia Hand standard grasps (i.e., power, lateral, and pinch grasps), hold the grasp for three seconds and release the object. This procedure was repeated 50 times for each object. These objects were: a cylinder, a square-based prism and a sphere for the power grasp, a thin card for the lateral grasp, a plate and a tripod for the pinch grasp. Except for the thin card, all the objects belong to the Southampton Hand Assessment Protocol (SHAP) kit [9]. To detect the touch event, we used an onset detection method based on the limit of detection (LoD). This method consisted of measuring whether the sensors signal overcame $\mu \pm 90\sigma$ during contact and release, where μ is the mean value and σ is the standard deviation of the baseline condition (i.e., when no load is applied). We selected this value due to the large signal-to-noise ratio of the sensor data. We assessed the event detection accuracy for each sensor across the different grasp types. Specifically, for each combination of sensor and grasp type, we determined the ratio between detected contact and release events with respect to the total number of occurred events (i.e., each grasp consists of one contact and one release event).

C. Dynamic evaluation of the sensorized thumb

The performance of the sensorized thumb was evaluated in dynamic scenarios through a pick and lift test (PLT) that involved the repetitive grasping, lifting, and replacement of a test object. Each pick and lift cycle consisted in reaching with the robotic hand the object positioned on a table, grasping it with a pinch grasp (i.e., using only the thumb and index fingers), lifting it to a specific height (30 cm), replacing it on the table and returning to the rest position. The test object was a cuboid (40 x 45 x 130 mm) integrating three load cells (SMD2551-012 S215, Strain Measurement Devices) to measure the forces exchanged during the manipulation task [9][16][18]. In particular, two load cells were placed on the lateral faces to measure the grip force applied by the thumb and index fingers, respectively, and one was placed below to measure the load force [14]. Data from the load cells was used to monitor the motor task and to synchronize the sensors signals with the manipulation phase. Because of the grasp type and the shape of the object, only the sensor S3 was monitored in this test. Data from the load cells and from the sensor was acquired with a DAQ board (USB 6001, National Instruments) through a custom GUI running on a PC. We tested two different conditions, described as follows.

Pre-programmed trajectories. This condition was performed to evaluate the accuracy of the sensors in detecting contact and release events in a simulated teleoperation procedure. The robotic follower was programmed to automatically execute a pre-defined trajectory that allowed to perform a pick and lift cycle, which was repeated 40 times. Accuracy was computed as the ratio between detected contact and release events with respect to the total number of occurred events, akin to Section

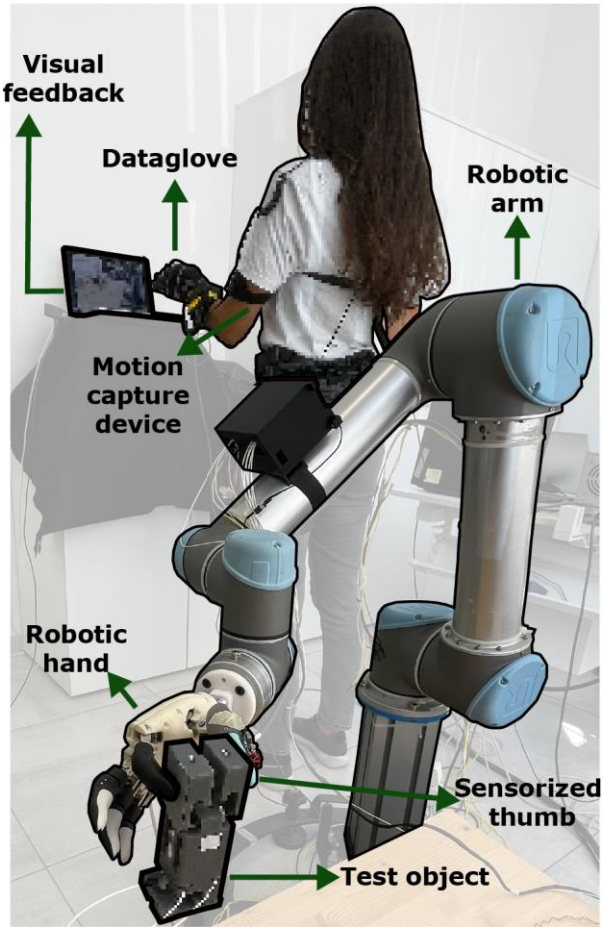

Fig. 5. Experimental setup for the pick and lift teleoperation test.

III.B. Furthermore, we recorded the rate of false positives counting the occurrence of additional (unwanted) detections and dividing this number by the total number of events.

Teleoperation. This condition aimed at evaluating the performances of the sensors during the execution of the PLT in a real teleoperation scenario. Eight right-handed healthy young adults were enrolled in the study (5 females and 3 males, aged 26.9±1.45 years old). All the participants were naïve to the purpose of the study and did not participate to previous experiments with the proposed system. This ensured that their background or experience did not bias our measures. Informed consent in accordance with the Declaration of Helsinki was obtained from each participant before conducting the experiment. The study was approved by the Ethical Committee of the Scuola Superiore Sant'Anna, Pisa, Italy (approval no. 10/2023). The experimental setup comprised the aforementioned teleoperation platform. The leader could control the robotic follower with a motion capture device (PN 32 V2, Perception Neuron) and a data glove (CyberGlove II, CyberGlove Systems). Leader and follower were interfaced through a custom software architecture developed in ROS. In details, the robotic fingers were controlled proportionally to the data glove outputs, while the inertial measurement units (IMUs) on the operator's hand allowed to control of the movement of the robotic arm in the operating space [18]. The whole system allowed the participants to remotely manipulate the test object, placed on a table about 10 cm far from the end effector of the follower system. Visual feedback about the status of the follower was provided to the participants by a webcam operating at 30 fps and directly interfaced with a monitor featuring a refresh rate of 60 Hz. Before the beginning of the experiment, the motion tracking system worn by the human leader was calibrated according to the producers' recommendations. Then, participants were asked to familiarize with the whole system by performing free movements, static grasps and pick and place movements for five minutes (Fig. **5**). After the familiarization phase, the participants were asked to use the telemanipulation setup to perform 30 repetitions of the PLT with the test object. The range of motion of the robotic arm was limited in the vertical plane and its velocity was limited up to 200 mm/s for safety reasons. Similarly, to the previous condition, we extracted contact and release detection accuracy and the rate of false positives. To further deepen this analysis, we classified false positives according to their cause, which mainly belong to two categories.

i) *Inertia.* Once the robotic hand grasped the object, sudden motions or vibrations of the robotic platform might lead to deformations of the thumb sensors. In fact, the fingertips of the robotic hand are covered with silicone and display a viscoelastic behavior, therefore any vibration that is transmitted to the test object is dampened by the fingertip, which gets deformed together with the embedded sensors. Video recordings of the tasks were visually inspected to identify the onset of vibrations or large accelerations when multiple detections occurred.

ii) *Grip force variation*. Unintentional finger motions of the participants while holding the test objects could cause grip force variation (ΔGF), generating undesired sensor responses recognized as a touch events. Load cells data were visually inspected to get this insight when multiple detections occurred.

IV. Results

A. Haptic display latency

Regarding the characterization of the haptic display latency, we measured a mean time delay between the detection of the touch event and the pneumatic inflation of the pocket across the

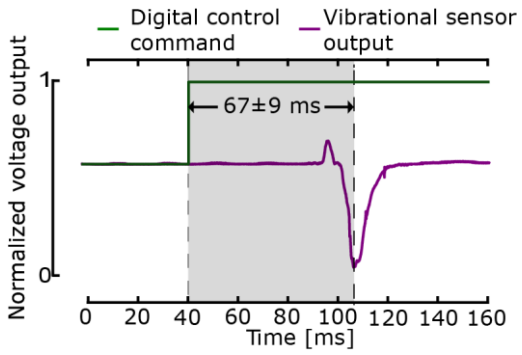

Fig. 6. Response of a pneumatic bag to contact detection of the PVDF-based sensor.

repetitions of 67±9 ms (Fig. **6**).

B. Static evaluation of the sensorized thumb

The touch-events detection accuracy of the sensorized thumb evaluated under static conditions showed extremely promising results. Specifically, each sensor accounted for an accuracy greater than 94% for the corresponding relevant grasp

TABLE I: CONTACT AND RELEASE EVENT DETECTION ACCURACY OF EACH SENSOR DURING STATIC GRASPS.

	S1			**S2**			**S3**		
	Pow	Lat	Pin	Pow	**Lat**	Pin	Pow	Lat	**Pin**
C	0.97	0.0	0.0	0.0	1.0	0.0	0.0	0.0	0.99
R	0.94	0.0	0.0	0.0	0.99	0.0	0.0	0.0	0.98

(i.e., S1 – power grasp, S2 – lateral grasp, S3 – pinch grasp, Fig. **7**), remaining unresponsive when executing the others (Table I).

C. Dynamic evaluation of the sensorized thumb

Pre-programmed trajectories. The system tested in a simulated teleoperation scenario (i.e., with the follower pre-programmed to perform pick and lift movements) proved capable of detecting all the contact events (100% detection accuracy) and 90% of the release events across the repetitions. The false positives rate was 37%.

Teleoperation. During telemanipulation, we obtained a contact detection accuracy of 100± [0 0] % (median± [interquartile range] across the participants), while the accuracy in detecting object release decreased to 86.4± [7.7 6.5] % (Fig. **8**a). We measured a rate of false positives for contact events of 10.5± [3.3 4.5] % due to inertia and of 6.5± [4.8 7.3] % due to ΔGF (Fig. **8**b). The rate of false positives for release events was instead 0± 0 %.

V. DISCUSSION

In this work, we presented a system for the detection of object contact and release events during telemanipulation and for the synchronous generation of haptic cues to the human leader. We leveraged PVDF-based piezoelectric sensors to capture the touch events, due to their response characteristics and their fast reaction time, assessed in our previous work [9]. Haptic cues were generated by a pneumatic textile-based haptic display, which showed low latency; this latency could be addressed in the future by reducing the length of the air tubing and using solenoid valves with shorter response times. Furthermore, in a teleoperation scenario, the haptic display latency is reduced when the webcam captures the scene immediately prior contact event. In this context, the user-perceived delay is equal to the difference between the haptic display latency and the reciprocal of the webcam frame rate. This is particularly encouraging, proving comparable to the state of the art where response times range between 40 and 300 ms [7].

Our findings also demonstrated that the sensors' shape and their placement on the thumb finger of a robotic hand were adequate. In fact, the sensorized finger showed great accuracy (>94%) in detecting contact and release events during static grasps for all the tested object, further proving the validity of the contact frequency maps that we used as reference to design the sensors [14]. Also, dynamic tests highlighted the great accuracy of the proposed system, which was only slightly lower than in static tests.

However, during the PLT with the pre-programmed robot, we noticed the occurrence of multiple detections in 37% of the trials. These detections were identified as false positives, likely resulting from the impact of the test object upon replacement on the table. Interestingly, this behavior was not observed during teleoperation, or at least occurred at lower frequencies. This discrepancy could be attributed to the nearly simultaneous replacement and release of the object when performed by the human operator.

On the other hand, although during teleoperation we obtained promising results, this test exposed some critical aspects. Expectedly, we observed lower accuracy when human leaders piloted the robotic follower with respect to when its motion followed predefined trajectories. This may be due to different known factors, such as a less smooth motion produced by the human operators, who also intrinsically introduce variability. We believe that mastering the teleoperation setup would improve the overall performance, which will be investigated in future studies. Finally, fine hand motions were required to perform the telemanipulation task, which were captured by motion tracking system. The accuracy of this motion tracking system might have introduced control instability, resulting in vibrations that ultimately may have increased false positive detections. Nonetheless, it should be noted that the accuracy of our sensing system ranged between

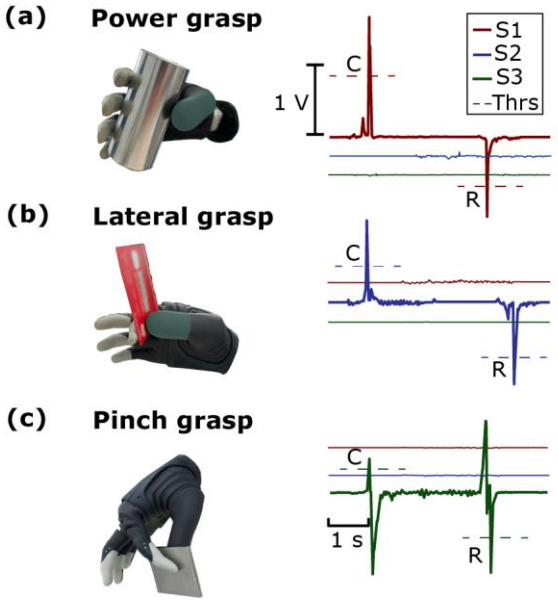

Fig. 7. Exemplar response of the sensorized thumb while grasping and releasing objects with (a) cylindrical, (b) lateral and (c) precision grasps. Dashed lines represent contact (C) and release (R) detection thresholds.

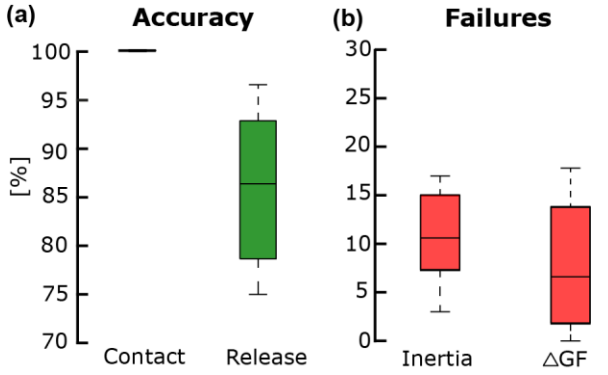

Fig. 8. Performance of the sensorized thumb during telemanipulation while performing the PLT task.

85% and 100%, and we measured a cumulative rate of false positives relatively small (<20%), encouraging further investigations [10].

Despite haptic feedback for telemanipulation is not a novel field [1][7][12], DESC policy has been scarcely explored, despite its potential being demonstrated in prosthetic [8] and in wearable applications [9][16]. DESC posits that the CNS subdivides manipulation tasks through discrete sensory events [8]. We believe that PVDF-based piezoelectric sensors are ideal for this application due to their sensitivity to transient stimuli, akin fast-adaptive mechanoreceptors [4]. In our previous studies, these sensors were integrated into a wearable device with the aim of restoring the sensorimotor function of the hand [9][16]. These sensors have already been integrated into robotic hands to record information about surface textures from a remote location and convey them to a user [19]. However, to the best of the authors' knowledge, these sensors have not been employed in real telemanipulation scenarios.

Our work expands the applicability of piezoelectric sensors to telemanipulation scenarios, especially thanks to their extremely low profile, which facilitates their integration in existing robotic platforms. Their versatility allowed us to strategically design their shape to capture contact on different locations of the finger, resulting capable of detecting touch events during different grasp types. On the other hand, these sensors are particularly sensitive to vibrations (in fact, they are mostly used as vibration sensors [16]), which may undesirably occur during telemanipulation. To tackle this, we designed a control algorithm based on a state machine, which proved effective without hampering the events detection accuracy.

Once the contact and release events are detected, a haptic display is necessary to convey corresponding stimuli to the user. Several strategies for providing feedback to the fingertips during teleoperation were proposed, mostly based on vibrotactile and electrotactile cues [2][9][10][12]. Despite the great versatility of vibrational actuators [5][8], their bulk and weight when placed on the fingertips can affect task performances [5]. Additionally, prolonged vibrations may interfere with the operator's ability to perceive other important sensory events [9][12], or have an anesthetizing effect [20]. Conversely, electrotactile feedback consists of delivering electrical stimulation to sensitive areas through surface electrodes [21]. To apply electrotactile feedback several aspects should be carefully assessed, to avoid issues such as skin irritation, burns, electric shock, and discomfort [10] , as well as muscle fatigue. As an alternative, textile-based pneumatic haptic displays have been recently proposed to deliver pressure cues to the user [22]. These systems leverage the lightness and conformability of pneumatic textile-based actuators, allowing to conveniently place the pneumatic components (pneumatic source, valves, controller, etc.) away from the user. To the best of the authors' knowledge, this is the first time that these actuators were proposed to provide feedback in telemanipulation. Additionally, offering localized sensory feedback could enhance telemanipulation performance, although it still represents a challenge [12]. The proposed haptic display can provide localized sensory feedback cues to arbitrary areas of the finger, while having a low profile and weight (3g).

Despite promising, our results are still preliminary. First, we tested only one type of grasp in the dynamic conditions, therefore further assessments should be carried out to validate the sensing elements and the control algorithm. Moreover, in-depth characterization of the haptic display must be performed, to fully capture its dynamic behavior. Moreover, future studies must be performed to validate whether our system, integrating the haptic display with the sensorized robotic hand, can enhance global telemanipulation performances. Research efforts will also be put in expanding the functionality of our system to capture and render continuous pressure information.

This study opens doors for the exploration of a novel haptic feedback policy in telemanipulation based on temporally discrete tactile events. With this goal in mind, we combined the versatility of piezoelectric touch sensors and textile-based actuators.

REFERENCES

[1] S. Haddadin, L. Johannsmeier, and F. D. Ledezma, "Tactile robots as a central embodiment of the tactile internet," *Proceedings of the IEEE*,vol. 107, no. 2, pp. 471–487, 2018.

[2] D. S. Pamungkas and K. Ward, "Tele-operation of a robot arm with electro tactile feedback," in *2013 IEEE/ASME International Conference on Advanced Intelligent Mechatronics*. IEEE, 2013, pp.704–709.

[3] N. Y. Lii *et al.*, "Exodex adam—a reconfigurable dexterous haptic user interface for the whole hand," *Frontiers in Robotics and AI*, vol. 8, p. 716598, 2022.

[4] R. S. Johansson and J. R. Flanagan, 'Coding and use of tactile signals from the fingertips in object manipulation tasks', *Nature Reviews Neuroscience*, vol. 10, no. 5, pp. 345–359, 2009.

[5] M. S. Islam and S. Lim, "Vibrotactile feedback in virtual motor learning: A systematic review," *Applied Ergonomics*, vol. 101, p.103694, 2022.

[6] A. Zangrandi *et al.*, 'Neurophysiology of slip sensation and grip reaction: insights for hand prosthesis control of slippage', *Journal of neurophysiology*, vol. 126, no. 2, pp. 477–492, 2021.

[7] C. Pacchierotti et al., 'Wearable Haptic Systems for the Fingertip and the Hand: Taxonomy, Review, and Perspectives', *IEEE Transactions on Haptics*, vol. 10, no. 4, pp. 580–600, 2017.

[8] C. Cipriani *et al.*, 'Humans can integrate feedback of discrete events in their sensorimotor control of a robotic hand', *Experimental brain research*, vol. 232, pp. 3421–3429, 2014.

[9] E. Vendrame *et al.*, "A wearable device for hand sensorimotor rehabilitation through augmented sensory feedback," in 2023 International Conference on Rehabilitation Robotics (ICORR), 2023, pp. 1–6.

[10]P. Kourtesis *et al.*, “Electrotactile feedback applications for hand and arm interactions:A systematic review, meta-analysis, and future directions,” *IEEE Transactions on Haptics*, 2022.

[11] M. Pinardi *et al.*, ‘Impact of supplementary sensory feedback on the control and embodiment in human movement augmentation’, *Communications Engineering*, vol. 2, no. 1, p. 64, 2023.

[12] C. Pacchierotti and D. Prattichizzo, ‘Cutaneous/Tactile Haptic Feedback in Robotic Teleoperation: Motivation, Survey, and Perspectives’, *IEEE Transactions on Robotics*, vol. 40, pp. 978–998, 2024.

[13] W. Heng, S. Solomon, and W. Gao, “Flexible electronics and devices as human–machine interfaces for medical robotics,” *Advanced Materials*, vol. 34, no. 16, p. 2107902, 2022.

[14] R. Guachi *et al.*, “Mechanical Integration of a Sensorized Skin in an Anthropomorphic Hand: Design pipeline and tests”, in *2024 10th IEEE RAS/EMBS International Conference for Biomedical Robotics and Biomechatronics (BioRob)*, 2024 (Accepted for publication).

[15] E. R. Kandel et al., Principles of neural science, vol. 4. McGraw-hill New York, 2000.

[16] E. Vendrame *et al.*, "An Instrumented Glove for Restoring Sensorimotor Function of the Hand Through Augmented Sensory Feedback," in *IEEE Transactions on Neural Systems and Rehabilitation Engineering*, vol. 32, pp. 2314-2323, 2024

[17] K. Englehart and B. Hudgins, ‘A robust, real-time control scheme for multifunction myoelectric control’, *IEEE Transactions on Biomedical Engineering*, vol. 50, no. 7, pp. 848–854, 2003

[18] L. Angelini *et al.*, “Self-collision avoidance in bimanual teleoperation using collisionik: algorithm revision and usability experiment,” in *2022 IEEE-RAS 21st International Conference on Humanoid Robots (Humanoids)*. IEEE,2022, pp. 112–118.

[19] P.H. Lin, S. Smith, ‘A teleoperation system for reproducing tactile perception using frequency channel segregation’, in *Haptic Interaction: Perception, Devices and Algorithms* 3, 2019, pp. 54–57.

[20] A. Fischer *et al.*, ‘Effects of Non-in Situ Vibrations on Hand Sensations: A Pilot Study’, in *Converging Clinical and Engineering Research on Neurorehabilitation IV: Proceedings of the 5th International Conference on Neurorehabilitation (ICNR2020)*, 2020, pp. 611–615.

[21] M. D’Alonzo *et al.*, ‘Electro-cutaneous stimulation on the palm elicits referred sensations on intact but not on amputated digits’, *Journal of neural engineering*, vol. 15, no. 1, p. 016003, 2017.

[22] V. Sanchez, C. J. Walsh, and R. J. Wood, ‘Textile technology for soft robotic and autonomous garments’, *Advanced functional materials*, vol. 31, no. 6, p. 2008278, 2021.